Composition Effect on Peptide Interaction with Lipids and Bacteria: Variants of C3a Peptide CNY21

Lovisa Ringstad,* Emma Andersson Nordahl,† Artur Schmidtchen,† and Martin Malmsten*
*Department of Pharmacy, Uppsala University, SE-751 23 Uppsala, Sweden; and †Department of Dermatology and Venereology, Lund University, Biomedical Center, SE-221 84 Lund, Sweden

ABSTRACT The effect of peptide hydrophobicity and charge on peptide interaction with model lipid bilayers was investigated for the C3a-derived peptide CNY21 by fluorescence spectroscopy, circular dichroism, ellipsometry, *z*-potential, and photon correlation spectroscopy measurements. For both zwitterionic and anionic liposomes, the membrane-disruptive potency for CNY21 variants increased with increasing net positive charge and mean hydrophobicity and was completely lost on elimination of all peptide positive charges. Analogous effects of elimination of the peptide positive net charge in particular were found regarding bacteria killing for both *Pseudomonas aeruginosa* and *Bacillus subtilis*. The peptides, characterized by moderate helix content both in buffer and when attached to the liposomes, displayed high adsorption for the net positively charged peptide variants, whereas adsorption was nonmeasurable for the uncharged peptide. That electrostatically driven adsorption represents the main driving force for membrane disruption in lipid systems was also demonstrated by a drastic reduction in both liposome leakage and peptide adsorption with increasing ionic strength, and this salt inactivation can be partly avoided by increasing the peptide hydrophobicity. This increased electrolyte resistance translates also to a higher antibacterial effect for the hydrophobically modified variant at high salt concentration. Overall, our findings demonstrate the importance of the peptide adsorption and resulting peptide interfacial density for membrane-disruptive effects of these peptides.

INTRODUCTION

Characterized by causing fast breakdown of bacterial membranes, antimicrobial peptides (AMPs) constitute a promising group of substances for combating bacterial infections, as resistance to conventional antibiotics is becoming an increasing problem, and ~800 AMPs of different origins have been identified today (1–6). Such AMPs have been isolated from plants (7,8) and insects (9) as well as domesticated animals (10), and many endogenous antimicrobial substances such as defensins, cathelicidins, and histatins have also been identified and shown to display multiple functions in the biological system (11–13).

A major challenge in the identification of AMPs for possible future clinical use is their selectivity, so that they are efficient against bacteria but do not affect human cells to any significant extent. Although there are discriminators between bacterial membranes and membranes of eukaryotic cells, such as the frequently higher charge density for bacteria and the presence of cholesterol in eukaryotic cells but not in bacteria (4,14), these discriminators provide only a rather limited selectivity of many AMPs. Given this, significant efforts have been directed to identifying AMPs that are efficient against bacteria but at the same time are nontoxic and do not interfere with eukaryotic cell membranes. Apart from screening for AMPs from various species, the use of synthetic combinatorial libraries for AMP identification has been attempted (1,15).

We have used a somewhat different approach for identifying efficient and low-toxicity AMPs, i.e., identification of peptides that can be generated through proteolytic degradation of endogenous proteins during bacterial infection. The reasoning behind this approach is that, provided that the amino acid sequences of the protein generating the peptide are evolutionarily well preserved, such peptide fragments should have low or only moderate, toxicity. Indeed, using this approach we have identified AMPs from human complement factor C3 (16), kininogen (17), and various extracellular matrix proteins (18) that are efficient against both Gram-positive and Gram-negative bacteria but at the same time display low human cell toxicity in terms of hemolysis and LDH release (16,17).

In a previous study the complement factor C3a was investigated and found to be bactericidal, thereby establishing a link between the adaptive and the innate immune system (16). Furthermore, it was shown that CNY21, the peptide sequence forming the 57–77 C-terminal of this protein (19) (Fig. 1), exerts antibacterial activity both in vitro and in a mouse model. In the study presented here, we investigate the antimicrobial activity of CNY21 further, together with the interaction between this peptide and model lipid membranes. In particular, we investigate the importance of electrostatic and hydrophobic interactions for the bactericidal activity of this peptide by selective amino acid substitutions to change peptide charge and hydrophobicity (Table 1). Furthermore, we attempt to obtain some information on the mechanism by which these peptides affect lipid membranes by comparing results from peptides with different compositional substitutions for well-defined model lipid

Submitted April 28, 2006, and accepted for publication August 28, 2006.

Address reprint requests to Lovisa Ringstad, Dept. of Pharmacy, Uppsala University, PO Box 580, SE-751 23 Uppsala, Sweden. E-mail: lovisa.ringstad@farmaci.uu.se.

0006-3495/07/01/87/12 $2.00

doi: 10.1529/biophysj.106.088161

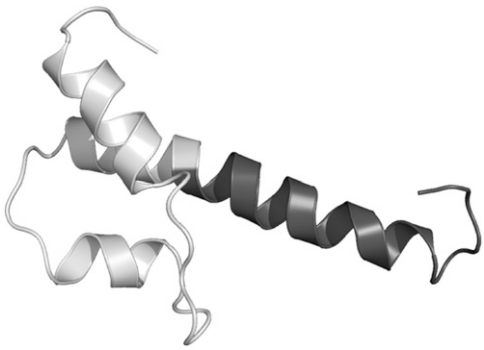

FIGURE 1 Structure of C3a, modified from Hugli (51). CNY21 constitutes the C-terminal part of C3a (amino acid residues 57–77, marked *black*).

membranes, using a combination of fluorescence spectroscopy, circular dichroism, ellipsometry, *z*-potential, and photon correlation spectroscopy.

MATERIALS AND METHODS

Materials

The peptides used in this investigation, CNY21, CNY21L, CNY21K, and CNY21R-S (Table 1), were synthesized by Innovagen (Lund, Sweden). Their purity was found to be >95% in all cases by MALDI-TOF MS analysis (Voyager, Applied Biosystems, Foster City, CA). 1,2-Dioleoyl-*sn*-glycero-3-phosphate (DOPA) (monosodium salt) and 1,2-dioleoyl-*sn*-glycero-3-phoshocholine (DOPC) were from Avanti Polar Lipids (Alabaster, AL) and of >99% purity; cholesterol (>99% purity), *n*-dodecyl-β-D-maltoside (DDM) (≥98% purity), Triton X-100, and poly-L-lysine (molecular mass 59 kDa and 170 kDa) were from Sigma-Aldrich (St. Louis, MO). 5(6)-Carboxyfluorescein (99% purity) was obtained from Acros Organics (Morris Plains, NJ). All other chemicals were of analytical grade, and water used was of Millipore Milli-Q Plus 185 ultrapure quality. All measurements were performed at pH 7.4 in 10 mM Tris-HCl buffer containing 5 mM glucose at 37°C, unless stated otherwise.

Surfaces

Silica surfaces for ellipsometry were prepared from polished silicon slides (Okmetic, Vantaa, Finland), oxidized to an oxide layer thickness of 30 nm. The slides were cleaned first in 25% NH_4OH, 30% H_2O_2, and H_2O (1:1:5, v/v) and then again in 32% HCl, 30% H_2O_2, and H_2O (1:1:5, v/v), both at 80°C for 5 min, which results in surfaces with an advancing contact angle of <10°. The surfaces were then stored in 95% ethanol. Just before use the surfaces were plasma treated for 5 min at 18 W in low-pressure residual air (0.2 mbar) (Harrick Plasma Cleaner, PDC-32G, Harrick Scientific, Ithaca, NY).

TABLE 1 Structure and properties of the peptides studied

Peptide	Sequence	Molecular weight (M)*	Isoelectric point*
CNY21	CNYITELRRQHARASHLGLAR	2465.8	10.69
CNY21L	CNYITELRRQLARASLLGLAR	2417.8	10.69
CNY21K	CNYITELRRQKARASKLGLAR	2447.8	10.94
CNY21R-S	CNYITELSSQHASASHLGLAS	2189.3	5.98

*Calculated from the peptide sequence by using the ProtParam tool available at http://www.expacy.org/tools/protparam.html.

Microorganisms

Pseudomonas aeruginosa 27.1 isolate was originally obtained from a patient with a chronic leg ulcer, and *Bacillus subtilis* ATCC isolate 6633 was obtained from The American Type Culture Collection (ATCC, Rockville, MD).

Radial diffusion assay

Radial diffusion assay (RDA) was performed as described previously (20). Bacteria (*B. subtilis* or *P. aerguinosa*) were both grown to midlogarithmic phase in 10 ml of 3% w/v trypticase soy broth (TSB) (Becton-Dickinson, Cockeysville, MD). The microorganisms were then washed with 10 mM Tris, pH 7.4. After this, 4×10^6 bacterial cfu was added to 5 ml of the underlay agarose gel, consisting of 1% (w/v) low-electroendosmosis type (low-EEO) agarose, 0.02% (v/v) Tween 20 (both Sigma-Aldrich), and 0.03% (w/v) TSB. The underlay formed by the latter was poured into Ø 85-mm petri dishes, and 4-mm-diameter wells were punched in the underlay after agarose solidification, after which a 6-μl sample was added to each well. Plates were then incubated at 37°C for 3 h to allow peptide diffusion. After this incubation time, the underlay gel was covered with 5 ml of molten overlay (6% TSB and 1% low-EEO agarose in dH_2O), and the peptide antimicrobial activity was visualized as clear zones around each well after 18–24 h of incubation at 37°C. Data presented from these experiments are expressed in terms of mean ($n = 18$ and 16 for *P. aeruginosa* and *B. subtilis*, respectively) diameter of the clear zones formed for the different peptides. The dose-response characteristics of RDA were used to determine the minimum effective concentration (MEC) of CNY21, CNY21L, and CNY21K against *P. aeruginosa*. The $\log_{10}$ concentrations of the peptides were plotted versus the respective diameter of the zone of clearance. Linear regression using least squares was used to estimate the MEC value, and it was determined by triplicate experiments by using eight serial twofold dilutions (starting at 512 μM) of the peptides.

Lactate dehydrogenase assay

HaCaT keratinocytes were grown in 96-well plates (3000 cells/well) in Dulbecco's Modified Eagle's Medium (DMEM) with 10% fetal calf serum (FCS) to confluency. The medium was removed, and the cells were washed with 100 μl DMEM. Then, 100 μl of the CNY21 peptides and LL-37 (60 μM) diluted in DMEM were added in triplicates to different wells of the plate. The LDH based TOX-7 kit (Sigma-Aldrich) was used for quantification of LDH release from the cells. Results given represent mean values from triplicate measurements.

Hemolysis

EDTA-blood was centrifuged at 800 *g* for 10 min, after which plasma and buffy coat were removed. The erythrocytes were then washed three times and resuspended in 5% PBS, pH 7.4. After this, the cells were incubated with end-over-end rotation for 1 h at 37°C in the presence of 60 μM peptide; 2% Triton X-100 (Merck, Stockholm, Sweden) served as positive control. The samples were then centrifuged at 800 *g* for 10 min. The absorbance of hemoglobin release was measured at $\lambda \approx 540$ nm and is expressed as percentage of Triton X-100–induced hemolysis. As negative control, the spontaneous leakage of hemoglobin during the same procedure was used. Results given represent mean values from triplicate measurements.

Liposome preparation

The liposomes investigated in this study were either anionic (DOPC/DOPA/cholesterol 30:30:40 mol/mol) or zwitterionic (DOPC/cholesterol 60:40 mol/mol). For both systems, lipid films were deposited on the inner walls of glass flasks by dissolving the phospholipid(s) and cholesterol in chloroform,

followed by evaporation under vacuum for 45 min at 60°C and subsequently in a vacuum oven (Lab-line, Melrose Park, NJ) at 30 in. Hg and room temperature overnight. After drying, the lipid mixtures were resuspended in 100 mM 5(6)-carboxyfluorescein (CF) in 10 mM Tris buffer, pH 7.4, and the solution was subjected to eight freeze-thaw cycles, where each cycle involved freezing in liquid nitrogen and heating to 60°C while vortexing. Unilamellar liposomes, largely free of multilamellar and defect liposomes (21,22) and of a 140-nm diameter (as confirmed by cryo-TEM and PCS), were produced by repeated extrusion through 100-nm polycarbonate membranes mounted in a LipoFast Basic extruder (Avestin, Mannheim, Germany). The liposomes thus generated were separated from untrapped CF by running the sample on a Sephadex G-25 column (Amersham Biosciences, Uppsala, Sweden) with Tris buffer as eluent.

Liposome leakage

Liposome leakage was studied by monitoring leakage-induced reduction of CF self-quenching. Specifically, CF release was determined by following the emitted fluorescence at 520 nm from a liposome dispersion (10 mM lipid in 10 mM Tris, pH 7.4, either with or without 150 mM NaCl added), with an absolute leakage scale obtained by disrupting the liposomes at the end of the experiment through addition of 0.05 wt % Triton X-100, thereby causing 100% release and dequenching of CF. A Spex fluorolog 1680 0.22-m double spectrometer (Instruments S.A. Group, Edison, NJ) was used, and all measurements were made in at least duplicate.

Peptide secondary structure

The peptide secondary structure was monitored by circular dichroism (CD) using a Jasco J-810 Spectropolarimeter (Jasco, Tokyo, Japan). The measurements were performed in the range 200–250 nm at 37°C under stirring in a 10-mm quartz cuvette and at a peptide concentration of 10 μM, both in buffer and in the presence of liposomes, the latter at a lipid concentration of 100 μM. The fraction of α-helical conformation was calculated from the recorded CD signal at 225 nm and from the corresponding signals of reference peptides in purely helical and random coil conformations, respectively; 100% α-helix and 100% random coil references were obtained from 0.133 mM (monomer concentration) poly-L-lysine (molecular mass 79 kDa) in 0.1 M NaOH and 0.1 M HCl, respectively (23,24). To account for the instrumental differences between measurements, the background value, detected at 250 nm, where no peptide signal is present, was subtracted. Signals from the bulk solution were also corrected for. All measurements were made in at least duplicate.

Peptide adsorption

Peptide adsorption to supported lipid bilayers was studied in situ by null ellipsometry, using an Optrel Multiskop (Optrel, Kleinmachnow, Germany) equipped with a 100-mW argon laser. All measurements were carried out at 532 nm and an angle of incidence of 67.66° in a 5-ml cuvette under stirring (300 rpm). Both the principles of null ellipsometry and the procedures used have been described extensively before (25–27). In brief, by monitoring the change in the state of polarization of light reflected at a surface in the absence and presence of an adsorbed layer, the mean refractive index (n) and layer thickness (d) of the adsorbed layer can be obtained. From the thickness and refractive index, the adsorbed amount (Γ) was calculated according to (28):

$$\Gamma = \frac{(n - n_0)}{dn/dc} d, \quad (1)$$

where dn/dc is the refractive index increment (0.154 cm^3/g (29,30)) and n_0 is the refractive index of the bulk solution. Corrections were routinely done for changes in bulk refractive index caused by changes in temperature and excess electrolyte concentration.

Zwitterionic bilayers were deposited by coadsorption from a mixed micellar solution containing 60:40 mol/mol DOPC/cholesterol and DDM, as described in detail previously (29). In brief, the mixed micellar solution was formed by addition of 19 mM DDM in water to DOPC/cholesterol dry lipid films, followed by stirring overnight, yielding a solution containing 97.3 mol % DDM, 1.6 mol % DOPC, and 1.1 mol% cholesterol. This micellar solution was added to the cuvette at 25°C, and the following adsorption monitored as a function of time. When adsorption had stabilized, rinsing with Milli-Q water at 5 ml/min was initiated to remove mixed micelles from solution and surfactant from the substrate (31). When this procedure is repeated and the concentration of the micellar solution is subsequently lowered, stable densely packed bilayers are formed with structural characteristics similar to those of bulk lamellar structures of the lipids (29,32).

Because subbilayer and patchy adsorption resulted from the above mixed micelle approach in the case of the anionic lipid mixture, supported lipid bilayers were generated from liposome adsorption in this case. DOPA/DOPC/cholesterol liposomes (30:30:40 mol/mol) were prepared as described above, but the dried lipid films were resuspended in Tris buffer only with no CF present. To avoid adsorption of peptide directly at the silica substrate through any defects of the supported lipid layer (see Fig. 8), poly-L-lysine (molecular mass 170 kDa) was preadsorbed from water before lipid addition to an amount of 0.045 $\pm$ 0.01 mg/m^2, followed by removal of nonadsorbed poly-L-lysine by rinsing with water at 5 ml/min for 20 min. Water in the cuvette was then replaced by buffer containing 150 mM NaCl, which was followed by addition of liposomes in buffer at a lipid concentration of 20 μM and subsequently rinsing with buffer (5 ml/min for 15 min) when the liposome adsorption had stabilized. The final layer formed had structural characteristics (thickness 40 $\pm$ 10 Å, mean refractive index 1.47 $\pm$ 0.026) similar to those of the zwitterionic bilayers, which suggests that a layer fairly close to a complete bilayer is formed. Again, the bilayer buildup was performed at 25°C.

After lipid bilayer formation, the temperature was raised, and the cuvette content was replaced by buffer at a rate of 5 ml/min over a period of 30 min. After stabilization for 40 min, peptide was added to a concentration of 0.01 μM, followed by three subsequent peptide additions to 0.1 μM, 0.5 μM, and 1 μM; in all cases the adsorption was monitored for 1 h. All measurements were made in at least duplicate.

Liposome *z*-potential

The z-potential of the liposomes was determined by electrophoretic mobility using a Zetasizer Nano ZS (Malvern Instruments, Worcestershire, UK). Measurements were performed at 25°C, due to air bubbles precluding measurements at 37°C, in disposable Zeta cells (Malvern Instruments). The lipid concentrations used were 40 μM for zwitterionic liposomes and 20 μM for anionic liposomes, respectively. These concentrations were chosen to obtain a count rate sufficiently high for the measurements. Peptide-to-lipid ratios were identical to those used in the leakage experiments. All measurements were made in at least triplicate 1 h after sample preparation.

Liposome size

The liposome diameter was measured by photon correlation spectroscopy using a Zetasizer Nano ZS (Malvern Instruments). All measurements were done at 173° scattering angle and 25°C in disposable plastic cuvettes. The lipid concentration was 40 μM for zwitterionic liposomes and 20 μM for anionic liposomes. Again, peptide-to-lipid ratios were chosen to be identical to those used in the leakage experiments. All measurements were made in triplicate 30 min after sample preparation.

RESULTS AND DISCUSSION

RDA analysis for bactericidal activity shows that all peptides investigated apart from CNY21R-S display bactericidal

effects for both Gram-negative and Gram-positive bacteria. Quantitatively, the bactericidal effects of the CNY21, CNY21K, and CNY21L peptides are of the same magnitude as those observed for the extensively studied and potent antimicrobial agent LL-37 (Fig. 2 *a*). In contrast to the benchmark peptide LL-37, however, the CNY21 peptides all display no measurable hemolytic activity above the background leakage negative control value (Fig. 3 *a*). Similarly, in contrast to LL-37, the CNY21 peptides all show negligible LDH release (Fig. 3 *b*). This membrane lysis specificity for bacteria over eukaryotic cells illustrates the desired selectivity for AMPs for possible therapeutic use, although clearly much more experimental support is needed to show the clinical relevance of the different peptides in vivo. More interesting for this investigation, however, is the comparison of the bactericidal effect of the different CNY21 variants. As can be seen in Fig. 2, *a* and *c*, increasing the peptide charge from +3 for CNY21 to +5 for CNY21K by two H→K substitutions results in a marginally increased bactericidal effect for both *P. aeruginosa* and *B. subtilis*, whereas the two H→L substitutions in CNY21L, rendering the peptide more hydrophobic (mean hydrophobicity according to the Kyte and Doolittle scale −0.68 and −0.01 for CNY21 and CNY21L, respectively) yield no effect for *P. aeruginosa* but the opposite effect for *B. subtilis*. (The differences in error bar sizes between *P. aeruginosa* and *B. subtilis* result from differences in growth variability between the strains and are thus not an effect of the peptides.) In this context, it should also be noted that the differences in effects of H→K and H→L substitutions for the two strains shown in Fig. 2 are not related to the Gram-positive/negative nature of the bacteria. Instead, we have investigated in total 10 different strains and found a strain variation of the order indicated by the two examples given in Fig. 2 that is not dependent on the Gram-positive/negative nature of the bacteria; hence, the strain differences seem not to be related to the presence of

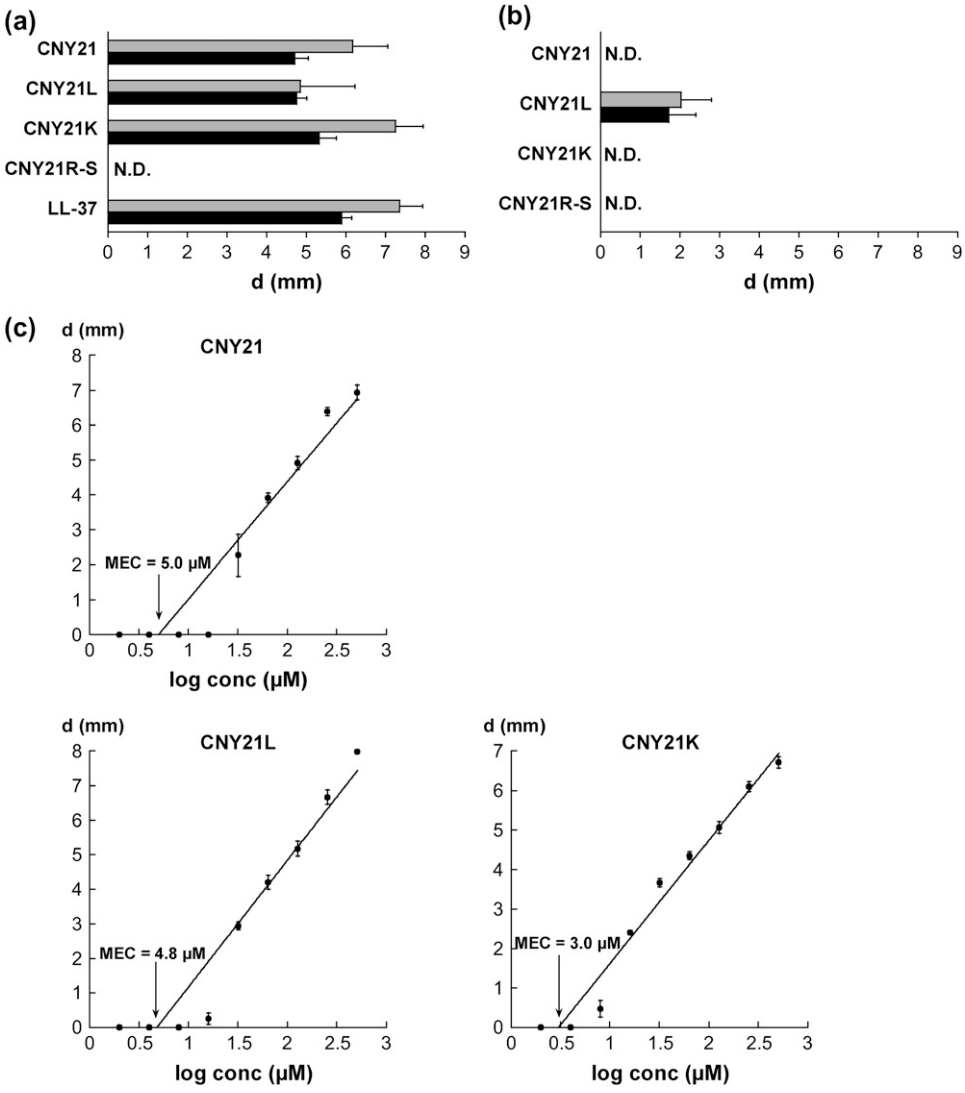

FIGURE 2 Bactericidal activity of the peptides against Gram-negative *P. aeruginosa* (*solid bars*) and Gram-positive *B. subtilis* (*shaded bars*) determined by RDA at a peptide concentration of 100 μM in 10 mM Tris, pH 7.4 (*a*) and in 10 mM Tris, pH 7.4 with additional 150 mM NaCl (*b*). The higher the diameter (*d*), the higher the bacterial growth inhibition. (*a*) Results on the extensively studied reference peptide LL-37 are also included for comparison. (*c*) The minimum effective concentration (MEC) studied by RDA for *P. aeruginosa*.

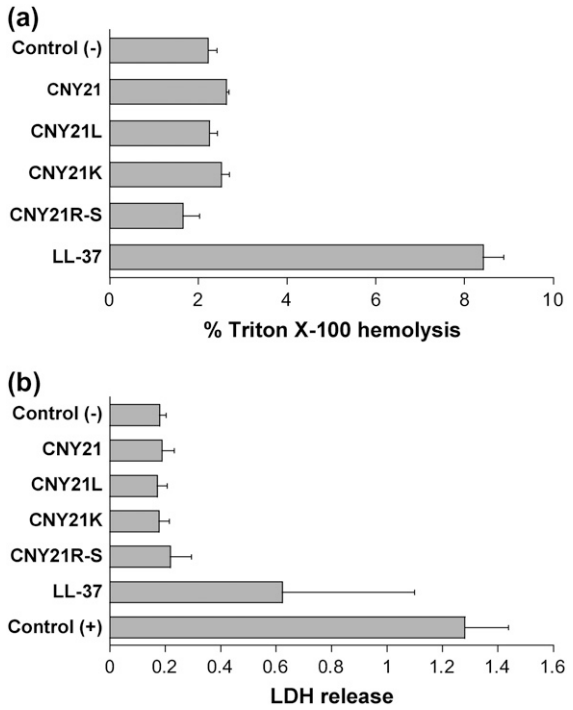

FIGURE 3 Peptide-induced hemolysis (*a*) and LDH release (*b*) at a peptide concentration of 60 μM. The absorbances for the positive and negative controls in the hemolysis were 4.96 $\pm$ 0.085 and 0.11 $\pm$ 0.01, respectively. Results on the extensively studied reference peptide LL-37 are also included for comparison.

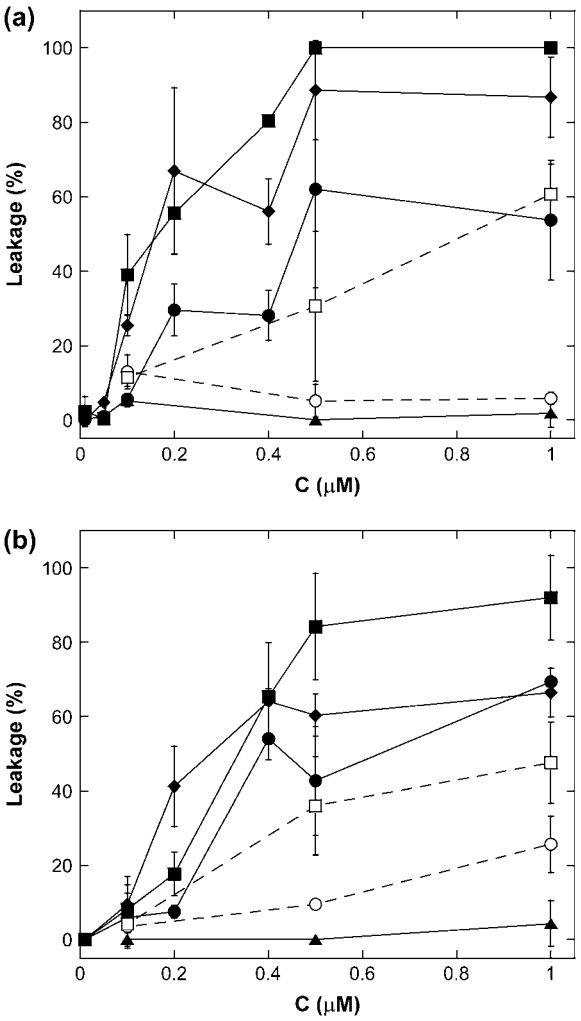

FIGURE 4 CF leakage from zwitterionic (*a*) and anionic (*b*) liposomes induced by CNY21 (●), CNY21L (■), CNY21K (♦), and CNY21R-S (▲). Peptide-induced CF leakage in buffer containing an additional 150 mM NaCl is also shown for CNY21 (○) and CNY21L (□).

additional lipid membrane and the presence of lipopolysaccharides in Gram-negative bacteria or to the higher charge density frequently observed for these (14). Nevertheless, all strains investigated show that eliminating the peptide net positive charge by four R→S substitutions results in complete elimination of the bactericidal effect of the peptide. The importance of a minimum electrostatic attraction between the peptide and the bacterial membrane is also illustrated by the peptides losing much of their bactericidal effect at high ionic strength, but the salt sensitivity may be reduced by introduction of a nonelectrostatic peptide-binding mechanism as in CNY21L (Fig. 2 *b*; see also discussion below).

The peptide composition influences leakage of CF from both zwitterionic and anionic liposomes to a significant extent. Increasing the hydrophobicity of the peptide by H→L substitution (CNY21L) resulted in increased leakage for both anionic and zwitterionic liposomes, as did increasing the peptide charge by H→K substitution. On the other hand, decreasing the peptide positive net charge by R→S substitution (CNY21R-S) totally eliminates peptide-induced CF leakage from both types of liposomes (Fig. 4). Interestingly, the leakage profile for zwitterionic liposomes is somewhat different for CNY21 and CNY21K compared to CNY21L (Fig. 4 *a*), indicating that there are differences in disruption mechanisms between these peptides. In the case of CNY21 and CNY21K, a possible onset of a second-state leakage induction is observed at 0.5 μM, whereas in the case of CNY21L, the leakage increases almost linearly with concentration until 100% leakage is obtained.

Although the leakage is lower from the anionic liposomes than from the zwitterionic ones in the case of CNY21K, the effects are not large and indicate that the membrane-disruptive effects are not drastically affected by the magnitude of the negative electrostatic potential in the range -10 mV (zwitterionic liposomes) to -31 mV (anionic liposomes). Given the quite similar results obtained for the zwitterionic and the anionic lipsomes, the selectivity of these peptides, displaying bactericidal effects but essentially no effect on eukaryotic cells with the assays used in this investigation, seems not to originate from the charge density difference between bacterial and eukaryotic cells alone, but rather from more complex interactions, where charge may well play a role. However, to fully investigate the role of

differences in charge density between bacteria and eukaryotic cell membranes for peptide selectivity, further work is needed, including lipid membranes not only varying in charge density, as in this case, but also more realistically monitoring differences in headgroup identity, presence or absence of cholesterol, length, asymmetry and degree of saturation of phospholipid acyl groups, etc.

Although this varies strongly between different systems, secondary structure transitions, notably coil→helix transitions, in some cases followed by peptide oligomerization, have been inferred to be important for the action of some AMPs (4,5,33–36). To obtain further mechanistic information on the mode of action of the currently investigated CNY21 variants, we therefore performed CD measurements in buffer and in the presence of anionic and zwitterionic liposomes. As shown in Table 2, the α-helix content is relatively low in buffer, and random coil is the dominating conformation. Furthermore, addition of zwitterionic or anionic liposomes did not affect the helix content to any significant degree in the case of CNY21, CNY21K, and CNY21R-S, and liposome leakage and CD measurements together show that major coil→helix transitions are not required for membrane disruption. In the presence of the anionic liposomes, the α-helix content is strongly increased in the case of CNY21L (Fig. 5), probably as a result of the lipid negative charges effectively acting as counterions, thereby stabilizing the helical conformation (37). A similar, but quantitatively smaller, preferential helix induction for the anionic liposomes is observed for CNY21, but because of the lower helix-forming tendency of the latter peptide, probably resulting from the lower hydrophobicity of this peptide compared to CNY21L, the magnitude of the helix induction as a result of the negatively charged surface is smaller for CNY21. Despite this much higher helical content for CNY21L in the case of the anionic liposomes, the membrane-disruptive effects of CNY21L are, in fact, slightly lower for the anionic than for the zwitterionic liposomes, which further suggests that helix formation is not a unique prerequisite for membrane disruption in the presently investigated systems. (Note that in the case of CNY21K and anionic liposomes, peptide-induced liposome flocculation, see below, prevented helix content from being reliably determined for this system.)

TABLE 2 Helix content of the peptides in solution and in presence of zwitterionic (DOPC/cholestrol 60:40 mol/mol) and anionic (DOPC/DOPA/cholestrol 30:30:40 mol/mol) liposomes

Peptide	Buffer	Zwitterionic liposomes	Anionic liposomes
CNY21	14 ± 1%	14 ± 2%	18 ± 2%
CNY21L	18 ± 2%	19 ± 4%	30 ± 8%
CNY21K	16 ± 2%	18 ± 1%	*
CNY21R-S	10 ± 4%	10 ± 6%	11 ± 5%

*CNY21K addition to the anionic liposomes resulted in flocculation, which precluded quantitative analysis of the peptide secondary structure.

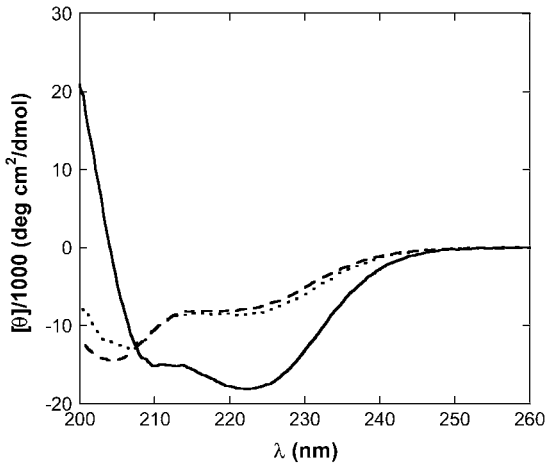

FIGURE 5 CD spectra for CNY21L in buffer (*dashed curve*) and in the presence of zwitterionic (*dotted curve*) and anionic (*solid curve*) liposomes.

Time-resolved adsorption curves for CNY21 at supported zwitterionic and anionic bilayers are presented in Fig. 6, showing an increased adsorption with increasing peptide concentration. CNY21, CNY21L, and CNY21K all display quite similar adsorption at zwitterionic and anionic bilayers (Figs. 7 and 8), but the adsorption of all these peptides is ~3 times higher at the anionic than the zwitterionic bilayers. This difference in peptide adsorption at the two types of lipid bilayers is related to the higher negative electrostatic potential for the anionic membrane, illustrated by the *z*-potential of the zwitterionic and the anionic liposomes without added peptide being -10 ± 3 mV and -31 ± 9 mV, respectively (Fig. 9). In contrast to CNY21, CNY21K, and CNY21L, CNY21R-S does not adsorb to any of the bilayers investigated (Figs. 7 and 8), which is in agreement with the negligible effect of addition of this peptide on liposome *z*-potential for both anionic and zwitterionic liposomes as well as with the lack of peptide-induced liposome leakage and bactericidal effect of this peptide. The finding that CNY21R-S, which has a marginally negative net charge (-1) under the conditions investigated, does not adsorb at any of the two bilayers, together with the finding of a much higher adsorption of CNY21, CNY21K, and CNY21L at anionic bilayers, indicate that electrostatic interactions constitute a major driving force for adsorption and also provide a requirement for peptide-induced liposome leakage and the bactericidal effect of these peptides. That electrostatic interactions play a role in adsorption is also evident when adsorption of CNY21, CNY21K, and CNY21L is compared at lower peptide concentrations (0.01 μM and 0.01 and 0.1 μM in case of zwitterionic and anionic bilayers, respectively) where adsorption of CNY21K, which has higher net positive charge (+5), is considerably higher than adsorption of CNY21 and CNY21L (+3). This is in agreement with CNY21K inducing higher leakage from anionic liposomes at lower concentrations compared to the

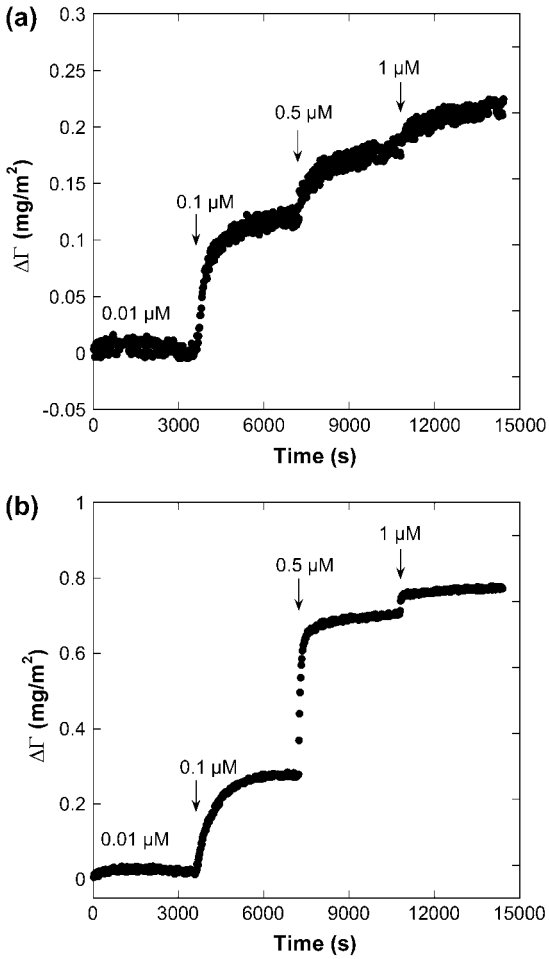

FIGURE 6 Time-resolved adsorption of CNY21 to supported zwitterionic (*a*) and anionic (*b*) bilayers. Peptide addition and final concentration in the cuvette after addition are indicated. Background adsorption for the lipid layer ($\Gamma = 4.27 \pm 0.006$ mg/m^2 and 4.48 ± 0.003 mg/m^2 for the zwitterionic and the anionic systems, respectively) is subtracted for clarity; $t = 0$ s corresponds to the time of the first peptide addition.

other peptides investigated (Fig. 4 *b*). However, at concentrations above 0.1 μM, no significant difference in adsorption is observed among CNY21L, CNY21, and CNY21K, even though the last is more charged, which suggests that electrostatic peptide-peptide interactions may constitute a limiting factor for peptide adsorption in a similar way as it does for many protein and polyelectrolyte systems (38).

In analogy to the adsorption results, the *z*-potential of the zwitterionic and anionic liposomes was not affected by addition of CNY21R-S, whereas CNY21 and CNY21K both resulted in a decreased negative *z*-potential for both the zwitterionic and the anionic systems (Fig. 9). Furthermore, given the higher net charge for CNY21K (+5) compared to CNY21 (+3), the finding that CNY21K is more potent than CNY21 in reducing the negative charge of the liposomes, despite the adsorption of CNY21K being very similar to that of CNY21 at both the anionic and the zwitterionic membrane (Figs. 7 and 8), is expected. Based on the *z*-potential of the liposomes in the absence of peptide and the effect of peptide on the *z*-potential, and using the adsorbed amounts from Figs. 7 and 8, we conclude that for CNY21K ~43% and 34% (for CNY21 50% and 14%, respectively) of the peptide charges are exposed at the plane of shear in the *z*-potential measurements for the zwitterionic and the anionic systems, respectively, the remainder being screened by counterion binding inside the shear plane and/or by peptide submersion into the bilayer.

To evaluate if peptide-induced liposome leakage correlated with liposome flocculation and coalescence, the liposome size was monitored (Fig. 10 *a*). Without added peptide the liposome size was 137 ± 9 nm and 140 ± 11 nm for zwitterionic and anionic liposomes, respectively. Addition of CNY21, CNY21L, and CNY21R-S did not have any major effect on liposome size. CNY21K, on the other hand, resulted in a drastically increased liposome size for the anionic but not the zwitterionic liposomes, an effect that was also seen at lower peptide-to-lipid ratios (Fig. 10 *b*). This shows that flocculation of anionic liposomes occurs in the presence of CNY21K at peptide-to-lipid ratios above 0.065, which may contribute to liposome leakage for this system. The liposome aggregation and possible coalescence were also reasons for not quantifying the peptide helix content for this system (Table 2) because material loss through flocculation, sedimentation/creaming, and/or attachment to cuvette walls could not be excluded in this case.

HIGH IONIC STRENGTH

Introducing additional 150 mM NaCl to the buffer reduces the effect of CNY21 and CNY21L in RDA (Fig. 2 *b*) and liposome leakage (Fig. 4) measurements drastically. Quantitatively, maximum leakage induction at high ionic strength for zwitterionic liposomes by CNY21 was <35% of that at low ionic strength for the anionic liposomes at 1 μM CNY21 and <10% for the zwitterionic liposomes (Fig. 4). A reduced capacity for liposome leakage induction is also observed for the more hydrophobic CNY21L, but this peptide nevertheless also displays considerable liposome leakage induction at high ionic strength, at maximum 50–60% leakage for both the zwitterionic and the anionic systems (Fig. 4). Mirroring trends were observed in the peptide adsorption at high ionic strength (Figs. 7 and 8). In the case of CNY21, no detectable adsorption to zwitterionic bilayers occurred in the presence of 150 mM NaCl, which should be compared to the negligible liposome leakage induction for the zwitterionic system at the same electrolyte concentration (Fig. 4 *a*). For the same peptide at the anionic membrane, adsorption was somewhat higher, as was liposome leakage induction, whereas CNY21L displays significant adsorption at high ionic strength to both lipid systems, amounting to ~80% and 30% of the adsorption of the same peptide to the anionic and zwitterionic lipid membrane at low ionic strength, respectively.

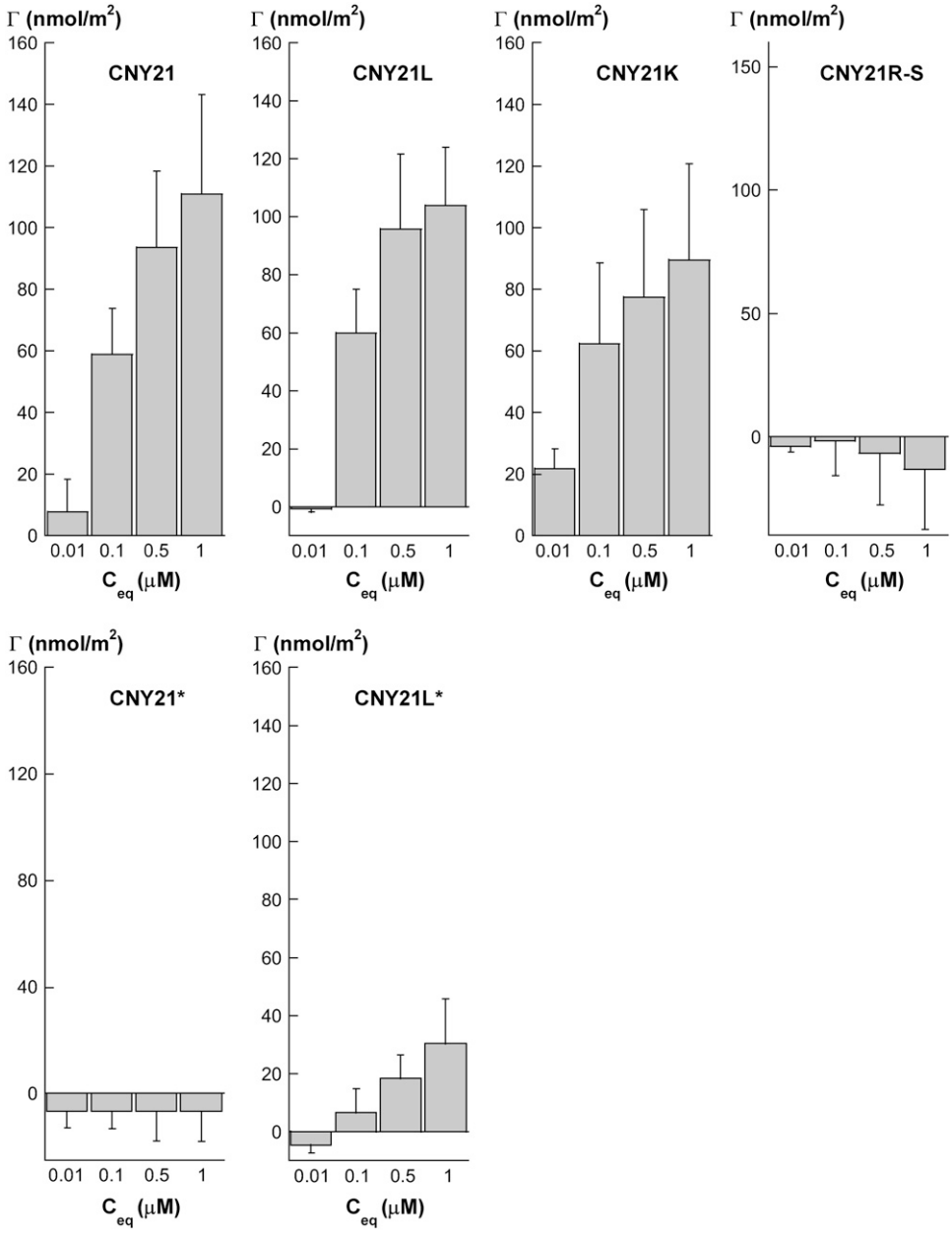

FIGURE 7 Peptide adsorption to zwitterionic bilayers measured by ellipsometry for CNY21, CNY21L, CNY21K, and CNY21R-S. CNY21*, CNY21L*, measured in buffer also containing 150 mM NaCl.

Although this is a less than ideal quantitative correlation with the fractional reduction in liposome leakage induction by CNY21L at high electrolyte concentration, the results nevertheless point once again to the close correlation between peptide adsorption density and membrane defect formation. The results also show that, although electrostatic interactions play an important role for the membrane-disrupting properties of CNY21, the importance of these, together with the electrolyte sensitivity of the peptide action on both liposomes and bacteria, can be reduced by introduction of a nonelectrostatic adsorption mechanism.

Although our results demonstrate the importance of peptide adsorption for lipid membrane disruption, the mechanisms by which this happens are still somewhat unclear. That adsorption to the lipid membrane is a requirement for membrane disruption is on one level an expected result given that the peptide concentration is sufficiently low to safely exclude the possibility of depletion-related effects commonly observed for colloidal systems containing high concentrations of nonadsorbing macromolecules (39). On the other hand, that membrane disruption depends on the extent of peptide adsorption above this threshold adsorption requirement is less obvious. There are several ways that peptide adsorption to lipid membranes can affect the integrity of the latter. Because CNY21, CNY21K, and CNY21L all have net positive charges, their adsorption reduces the net negative electrostatic potential of the liposomes, as seen, e.g., in the *z*-potential measurements (Fig. 9), which could result in

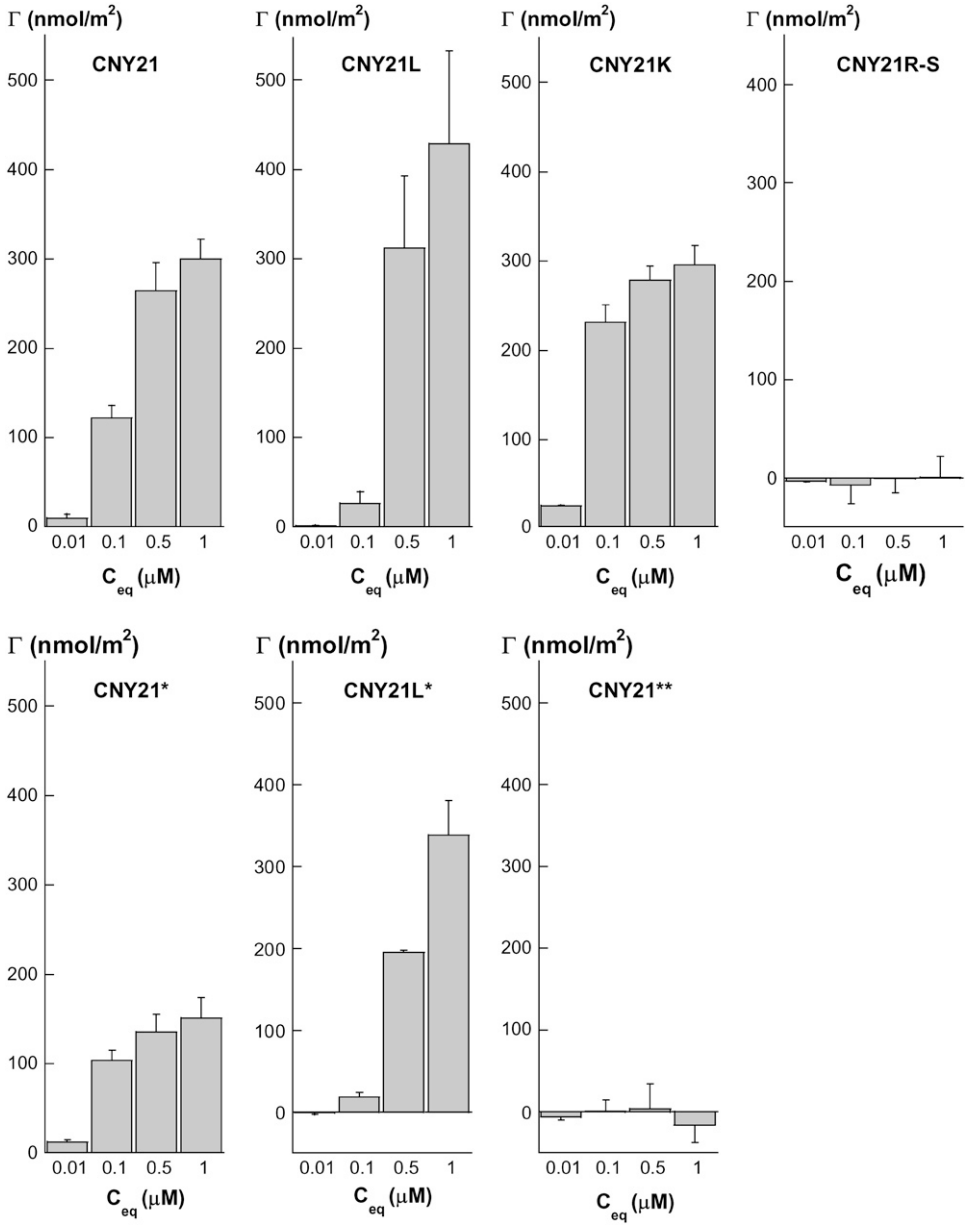

FIGURE 8 Peptide adsorption to anionic bilayers measured by ellipsometry for CNY21, CNY21L, CNY21K, and CNY21R-S. CNY21*, CNY21L*, measured in buffer also containing 150 mM NaCl. Also shown is the adsorption of CNY21 to silica coated by 0.045 ± 0.01 mg/m^2 poly-L-lysine (CNY21**).

liposome flocculation and coalescence. Because particle growth was observed for CNY21K and the anionic liposome, contributions from liposome aggregation and flocculation to leakage induction may be a factor to consider in this system. For all other systems investigated, however, no signs of significant particle growth were observed, indicating that such large-scale colloidal effects are of marginal importance for the peptide-induced liposome leakage. Similarly, liposome-to-micelle transitions, observed for some peptides in liposome systems (40,41) as well as for liposomes exposed to cationic single-chain surfactants (42,43) may be discarded based on the liposome size results. Furthermore, although helix induction is observed on peptide inclusion in the liposome, notably for CNY21L and the anionic liposomes, there is no clear correlation between helix and leakage inductions, and except for that one case, the helix content of the peptides in both types of liposomes is relatively low. Mechanisms based on membrane-bound oligomers of peptide helices observed for some AMPs (44–46) seem less likely. To exclude the presence of such mechanisms with absolute certainty, however, will require further investigation. Instead, it seems that some types of packing defects are formed around the adsorbed peptide molecules. Such defects are not driven by a buildup of global positive electrostatic potential on peptide adsorption, as for some lipid-cationic surfactant systems (42,43), which is clearly demonstrated by the *z*-potential data. Instead, a possible mechanism for the adsorption-related membrane rupture may be membrane

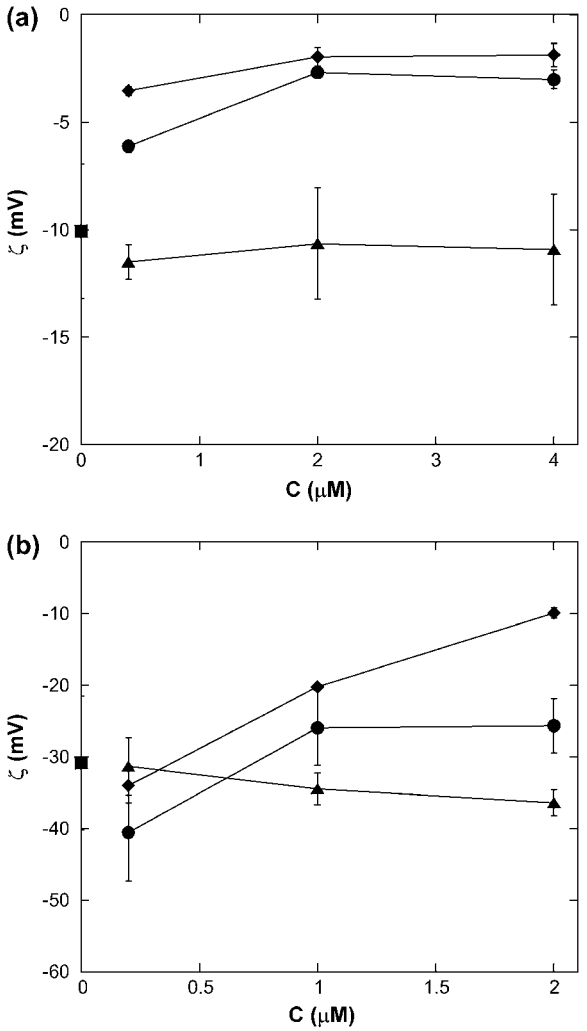

FIGURE 9 *z*-Potential for zwitterionic (*a*) and anionic (*b*) liposomes in presence of CNY21 (●), CNY21K (♦), and CNY21R-S (▲). The *z*-potential of the liposomes without added peptides is also shown (■).

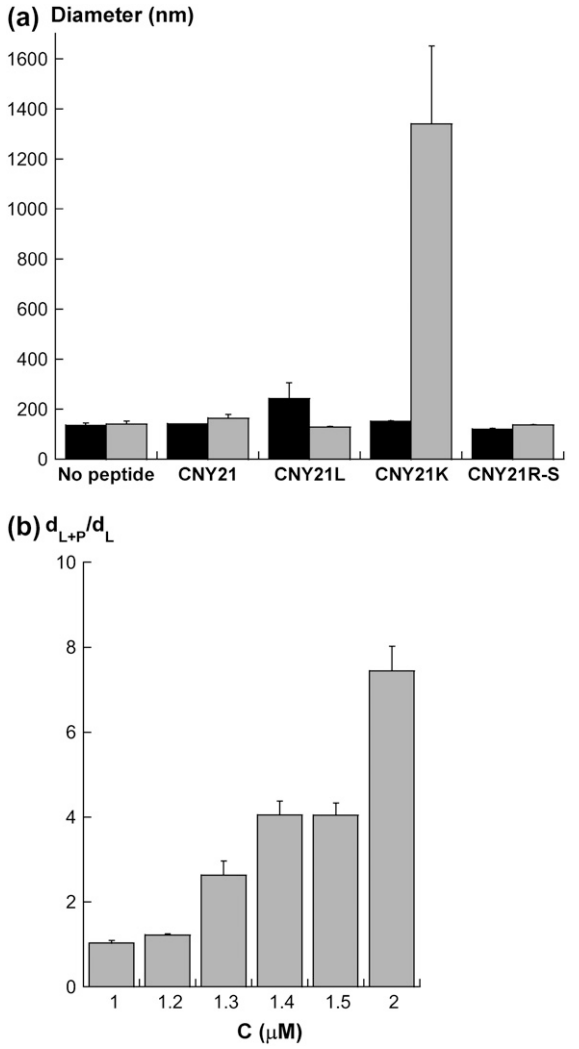

FIGURE 10 (*a*) Liposome size presented as Z-average diameter for zwitterionic (*solid bars*) and anionic liposomes (*shaded bars*) without added peptide and with CNY21, CNY21L, CNY21K, and CNY21R-S at a peptide/lipid molar ratio of 0.1, i.e., 4 μM and 2 μM peptide in case of zwitterionic and anionic liposomes, respectively. (*b*) Effect of the CNY21K concentration on the size of the anionic liposomes 30 min after peptide addition, presented as the ratio between liposome diameter before (d_L) and after (d_{L+P}) peptide addition.

thinning caused by peptide incorporation in the headgroup region of the lipid bilayer, resulting in an effective increase in the area per lipid molecule, which in turn allows for a stretching relaxation on the aliphatic chains of the phospholipids (47–50). For the supported bilayers, however, we observe no major changes in the adsorbed layer thickness after addition of CNY21, CNY21K, and CNY21R-S. CNY21L adsorption, on the other hand, resulted in an increased thickness of the anionic bilayers by ~20% after the final peptide addition (data not shown). Hence, although this might differ among AMPs, no experimental results currently available support such a membrane-thinning mechanism for bilayer disruption caused by the peptides investigated in this study. Also other mechanisms are possible, e.g., electrostatically driven packing defects around each adsorbed peptide molecule. Further work to elucidate these mechanisms is needed, and it is currently under way.

CONCLUSIONS

Peptide composition is important for the antibacterial properties of CNY21 variants and also for their membrane disruption in unilamellar liposomes. Increasing the positive charge or hydrophobicity of the peptide results in an increased membrane-disruptive capacity toward both zwitterionic and anionic liposomes, whereas eliminating the peptide net positive charge results in elimination of membrane-lysing capacity of the peptide. These effects are related to the adsorption of the peptide at the lipid bilayers, but the peptide secondary structure seems to play a less important role in the membrane defect formation. The adsorption, in turn,

is dominated by electrostatic peptide-lipid interactions, although hydrophobic interactions also play a role, clearly demonstrated by CNY21L. Even though the detailed mechanism by which adsorption of these structurally relatively disordered peptides results in defect formation is unknown at present, the results point toward the formation of local packing defects (''counterion binding'' at the expense of optimal lamellar packing) around the peptide molecules caused by the charges they carry. A surprisingly good correlation is observed between liposomes and bacteria, indicating that lipid bilayer rupture is a key mechanism of the antibacterial action of these peptides.

We thank Ms. Lotta Wahlberg and Ms. Mina Davoudi for expert technical assistance, Professor Lennart Bergström for putting the *z*-potential and photon correlation spectroscopy instrumentation to our disposal, Jovice Boon-Sing Ng for assistance with the *z*-potential measurements, and Dr. Björn Walse for help with Fig. 1.

This work was supported by grants from the Swedish Research Council (projects 13471 and 621-2003-4022), the Royal Physiographic Society in Lund, the Welander-Finsen, Thelma-Zoegas, Groschinsky, Crafoord, Åhlen, Alfred Österlund, Lundgrens, Lions, and Kock Foundations, The Swedish Government Funds for Clinical Research, and DermaGen AB.

REFERENCES

1. Lohner, K., and S. E. Blondelle. 2005. Molecular mechanisms of membrane perturbation by antimicrobial peptides and the use of biophysical studies in the design of novel peptide antibiotics. *Comb. Chem. High Throughput Screen.* 8:241–256.
2. Papo, N., and Y. Shai. 2003. Can we predict biological activity of antimicrobial peptides from their interactions with model phospholipid membranes? *Peptides.* 24:1693–1703.
3. Shai, Y. 2002. Mode of action of membrane active antimicrobial peptides. *Biopolymers.* 66:236–248.
4. Toke, O. 2005. Antimicrobial peptides: New candidates in the fight against bacterial infections. *Biopolymers.* 80:717–735.
5. Zasloff, M. 2002. Antimicrobial peptides of multicellular organisms. *Nature.* 415:389–395.
6. Tossi, A. http://www.bbcm.univ.trieste.it/~tossi/pag2.htm.
7. Colilla, F. J., A. Rocher, and E. Mendez. 1990. γ-Purothionins: amino acid sequence of two polypeptides of a new family of thionins from wheat endosperm. *FEBS Lett.* 270:191–194.
8. Mendez, E., A. Moreno, F. Colilla, F. Pelaez, G. G. Limas, R. Mendez, F. Soriano, M. Salinas, and C. de Haro. 1990. Primary structure and inhibition of protein synthesis in eukaryotic cell-free system of a novel thionin, gamma-hordothionin, from barley endosperm. *Eur. J. Biochem.* 194:533–539.
9. Bulet, P., C. Hetru, J.-L. Dimarcq, and D. Hoffmann. 1999. Antimicrobial peptides in insects; structure and function. *Dev. Comp. Immunol.* 23:329–344.
10. Brogden, K. A., M. Ackermann, P. B. McCray Jr., and B. F. Tack. 2003. Antimicrobial peptides in animals and their role in host defences. *Int. J. Antimicrob. Agents.* 22:465–478.
11. De Smet, K., and R. Contreras. 2005. Human antimicrobial peptides: defensins, cathelicidins and histatins. *Biotechnol. Lett.* 27:1337–1347.
12. Ganz, T. 2005. Defensins and other antimicrobial peptides: A historical perspective and an update. *Comb. Chem. High Throughput Screen.* 8:209–217.
13. Brown, K. L., and R. E. Hancock. 2006. Cationic host defence (antimicrobial) peptides. *Curr. Opin. Immunol.* 18:24–30.
14. Madigan, M. T., J. M. Martinko, and J. Parker. 1997. Brock biology of microorganisms. Prentice-Hall, Upper Saddle River, NJ.
15. Hilpert, K., R. Volkmer-Engert, T. Walter, and R. E. W. Hancock. 2005. High-throughput generation of small antibacterial peptides with improved activity. *Nat. Biotechnol.* 23:1008–1012.
16. Andersson Nordahl, E., V. Rydengård, P. Nyberg, D. P. Nitsche, M. Mörgelin, M. Malmsten, L. Björck, and A. Schmidtchen. 2004. Activation of the complement system generates antibacterial peptides. *Proc. Natl. Acad. Sci. USA.* 101:16879–16884.
17. Andersson Nordahl, E., V. Rydengård, M. Mörgelin, and A. Schmidtchen. 2005. Domain 5 of high molecular weight kininogen is antibacterial. *J. Biol. Chem.* 280:34832–34839.
18. Malmsten, M., M. Davoudi, and A. Schmidtchen. 2006. Bacterial killing by heparin-binding peptides from PRELP and thrombospondin. *Matrix Biol.* 25:294–300.
19. Lu, Z. X., K. F. Fok, B. W. Erickson, and T. E. Hugli. 1984. Conformational analysis of COOH-terminal segments of human C3a. Evidence of ordered conformation in an active 21-residue peptide. *J. Biol. Chem.* 259:7367–7370.
20. Lehrer, R. I., M. Rosenman, S. S. Harwig, R. Jackson, and P. Eisenhauer. 1991. Ultrasensitive assays for endogenous antimicrobial polypeptides. *J. Immunol. Methods.* 137:167–173.
21. MacDonald, R. C., F. D. Jones, and R. Qiu. 1994. Fragmentation into small vesicles of dioleoylphosphatidylcholine bilayers during freezing and thawing. *Biochim. Biophys. Acta.* 1191:362–370.
22. Traikia, M., D. E. Warschawski, M. Recouvreur, J. Cartaud, and P. F. Devaux. 2000. Formation of unilamellar vesicles by repetitive freeze-thaw cycles: characterization by electron microscopy and ^{31}P-nuclear magnetic resonance. *Eur. Biophys. J.* 29:184–195.
23. Greenfield, N. 1969. Computed circular dichroism spectra for the evaluation of protein conformation. *Biochemistry.* 8:4108–4116.
24. Sjögren, H., and S. Ulvenlund. 2005. Comparison of the helix-coil transition of a titrating polypeptide in aqueous solutions and at the air-water interface. *Biophys. Chem.* 116:11–21.
25. Azzam, R. M. A., and N. M. Bashara. 1989. Ellipsometry and polarized light. North Holland Publishing Company, Amsterdam.
26. Landgren, M., and B. Jönsson. 1993. Determination of the optical properties of Si/SiO_2 surfaces by means of ellipsometry, using different ambient media. *J. Phys. Chem.* 97:1656–1660.
27. Malmsten, M. 1994. Ellipsometry studies of protein layers adsorbed at hydrophobic surfaces. *J. Colloid Interface Sci.* 166:333–342.
28. de Feijter, J. A., J. Benjamins, and F. A. Veer. 1978. Ellipsometry as a tool to study the adsorption of synthetic and biopolymers at the air-water interface. *Biopolymers.* 17:1759–1772.
29. Tiberg, F., I. Harwigsson, and M. Malmsten. 2000. Formation of model lipid bilayers at the silica-water interface by co-adsorption with non-ionic dodecyl maltoside surfactant. *Eur. Biophys. J.* 29:196–203.
30. Vacklin, H. P., F. Tiberg, G. Fragneto, and R. K. Thomas. 2005. Phospholipase A_2 hydrolysis of supported phospholipid bilayers: a neutron reflectivity and ellipsometry study. *Biochemistry.* 44:2811–2821.
31. Ringstad, L., A. Schmidtchen, and M. Malmsten. 2006. Effect of peptide length on the interaction between consensus peptides and DOPC/DOPA bilayers. *Langmuir.* 22:5042–5050.
32. Vacklin, H. P., F. Tiberg, and R. K. Thomas. 2005. Formation of supported phospholipid bilayers via co-adsorption with β-D-dodecyl maltoside. *Biochim. Biophys. Acta.* 1668:17–24.
33. Matsuzaki, K. 1998. Magainins as paradigm for the mode of action of pore forming polypeptides. *Biochim. Biophys. Acta.* 1376:391–400.
34. Oren, Z., J. C. Lerman, G. H. Gudmundsson, B. Agerberth, and Y. Shai. 1999. Structure and organization of the human antimicrobial peptide LL-37 in phospholipid membranes: relevance to the molecular basis for its non-cell-selective activity. *Biochem. J.* 341:501–513.
35. Pouny, Y., and Y. Shai. 1992. Interaction of D-amino acid incorporated analogues of pardaxin with membranes. *Biochemistry.* 31:9482–9490.

36. Tossi, A., L. Sandri, and A. Giangaspero. 2000. Amphiphatic, α-helical antimicrobial peptides. *Biopolymers*. 55:4–30.

37. Nilsson S., L. Piculell, and B. Jönsson. 1989. Helix-coil transitions of ionic polysaccharides analyzed within the Poisson-Boltzmann cell model. 1. Effects of polyion concentration and counterion valency. *Macromolecules*. 22:2367–2375.

38. Fleer, G. J., M. A. Cohen Stuart, J. M. H. M. Scheutjens, T. Cosgrove, and B. Vincent. 1993. Polymers at interfaces. Chapman & Hall, London.

39. Napper, D. H. 1983. Polymeric stabilization of colloidal dispersions. Academic Press, London.

40. Heerklotz, H., and J. Seelig. 2001. Detergent-like action of the antibiotic peptide surfactin on lipid membranes. *Biophys. J*. 81:1547–1554.

41. Monette, M., and M. Lafleur. 1996. Influence of lipid chain unsaturation on melittin-induced micellization. *Biophys. J*. 70:2195–2202.

42. Edwards, K., J. Gustafsson, M. Almgren, and G. Karlsson. 1993. Solubilization of lecithin vesicles by a cationic surfactant: intermediate structures in the vesicle-micelle transition observed by cryo-transmission electron microscopy. *J. Colloid Interface Sci*. 161:299–309.

43. Gustafsson, J., G. Orädd, and M. Almgren. 1997. Disintergration of the lecithin lamellar phase by cationic surfactants. *Langmuir*. 13:6956–6963.

44. Feder, R., A. Dagan, and A. Mor. 2000. Structure-activity relationship study of antimicrobial dermaseptin S4 showing the consequences of peptide oligomerization on selective cytotoxicity. *J. Biol. Chem*. 275: 4230–4238.

45. Nomura, K., G. Corzo, T. Nakajima, and T. Iwashita. 2004. Orientation and pore-forming mechanism of a scorpion pore-forming peptide bound to magnetically oriented lipid bilayers. *Biophys. J*. 87:2497–2507.

46. Strahilevitz, J., A. Mor, P. Nicolas, and Y. Shai. 1994. Spectrum of antimicrobial activity and assembly of dermaseptin-b and its precursor form in phospholipid membranes. *Biochemistry*. 33:10951–10960.

47. Chen, F.-Y., M.-T. Lee, and H. W. Huang. 2003. Evidence for membrane thinning effect as the mechanism for peptide-induced pore formation. *Biophys. J*. 84:3751–3758.

48. He, K., S. J. Ludtke, W. T. Heller, and H. W. Huang. 1996. Mechanism of alamethicin insertion into lipid bilayers. *Biophys. J*. 71:2669–2679.

49. Heller, W. T., A. J. Waring, R. I. Lehrer, T. A. Harroun, T. M. Weiss, L. Yang, and H. W. Huang. 2000. Membrane thinning effect of the β-sheet antimicrobial protegrin. *Biochemistry*. 39:139–145.

50. Ludtke, S., K. He, and H. Huang. 1995. Membrane thinning caused by magainin 2. *Biochemistry*. 34:16764–16769.

51. Hugli, T. E. 1989. Structure and function of C3a anaphylatoxin. *Curr. Top. Microbiol. Immunol*. 153:181–208.